Electrochemistry of Conductive Polymers. 34. Two-Dimensional Correlation Analysis of Real-Time Spectroelectrochemical Data for Aniline Polymerization

Sun-Young Hong,[†] Young Mee Jung,[‡] Seung Bin Kim,[‡] and Su-Moon Park*[,†,‡,§]

School of Environmental Science and Engineering, Department of Chemistry, and Center for Integrated Molecular Systems, Pohang University of Science and Technology, Pohang 790-784, Korea

Received: August 22, 2004; In Final Form: December 30, 2004

Electrochemical polymerization of aniline has been studied using real-time spectroelectrochemical experiments conducted concurrently with potentiodynamic scans in a nitric acid electrolyte with its pH adjusted to 0.50. Two-dimensional correlation spectral analysis and subsequent extraction of pure component spectra as well as their relative concentration profiles from complex spectroelectrochemical data employing the alternating least-squares regression iteration-based self-modeling curve resolution method led to positive identification of intermediate species. A conclusion was reached on the polymerization reaction mechanism based on these intermediate species and how their concentrations increased or decreased during the potential scans. The mechanism thus concluded represents a summary of a current understanding of the aniline polymerization reaction.

Introduction

A large number of studies have been reported on the synthesis and characterization of polyaniline (PAn) since it has been known to be an electrically conducting polymer.[1] PAn is prepared rather straightforwardly by chemical and electrochemical methods, readily converted between conductive and insulating forms, and reasonably stable in its conductive form. Much attention has been paid to the elucidation of its polymerization mechanism[2] because PAn represents one of the best examples that can be obtained by a simple oxidation reaction. Nevertheless, the mechanisms of its formation and growth are still controversial after a number of studies conducted on it. The controversies arise from the fact that the reaction is made of a series of complex ECE (electrochemical−chemical−electrochemical) reactions, leading to significant confusions on the part of interpretation of the current responses to potential excitation and/or vice versa.[2a−c,f] Other techniques supplementing electrochemical experiments such as spectroelectrochemical and electrochemical quartz crystal microbalance (EQCM) studies provided only limited aids to these efforts because the spectral or EQCM signals resulting from aniline oxidation and products thereof are either heavily convoluted or do not offer species selectivity.[2e,g]

The first exhaustive studies on the mechanism of aniline oxidation have been carried out by Adams et al. as early as in the 1960s,[2a,b] well before PAn was recognized as a conducting polymer. Adams et al. reported that two dimers, benzidine and *N*-phenyl-*p*-phenylene diamine (PPD), were produced as oxidation products in different proportions depending on the pH of the medium when a small amount of aniline was oxidized, which does not lead to polymerization. Later, we identified these species as major intermediate species in the aniline polymerization reaction employing spectroelectrochemical studies,[2e,g] but the spectra obtained were too complex for us to reach an unambiguous conclusion on the PAn growth mechanism even though we were able to identify these species from their absorption peaks.

Chemometrics applied to a curve resolution problem is a well-recognized technique for the analysis of complex spectroscopic data sets. Combination of two-dimensional (2D) correlation spectroscopy[3] with the alternating least-squares (ALS) regression iteration-based self-modeling curve resolution (SMCR)[4] analysis offers a very powerful tool for interpreting highly convoluted spectra. This technique utilizes the nonnegativity constraints for spectral intensities and concentrations by use of the intensities of distinct cross peaks located at the off-diagonal positions of an asynchronous 2D correlation spectrum. The ALS-based SMCR analysis allows the pure component spectra and concentration profiles to be extracted from a large number of spectra recorded with an external perturbation applied. The 2D correlation spectroscopy has been applied extensively to the analysis of spectral data sets obtained during the observation of a system under a given external perturbation.[5] It enables the enhancement of the spectral resolution by spreading peaks along the two dimensions, simplification of complex spectra consisting of many overlapped peaks, establishment of unambiguous assignments of bands selectively coupled by various interaction mechanism, and identification of the sequence of the spectral intensity changes by an external perturbation. Moreover, 2D correlation spectroscopy has been applied to analyze systematic patterns of subtle spectral changes induced by an external perturbation that are not readily noticeable in conventional one-dimensional spectra. Recently, we have demonstrated that the highly convoluted spectrum of two very similar spectra can be successfully resolved into their component spectra.[6]

In the present study, we attempt to completely resolve the complex spectra obtained during oxidation of aniline during the first potentiodynamic cycle and the subsequent polyaniline growth during the following potential cycles, employing two-dimensional correlation analysis with the ALS regression iteration-based SMCR analysis. We then shed light on the

* Corresponding author. Phone: +82-54-279-2102. Fax: +82-54-279-3399. E-mail: smpark@postech.edu.
[†] School of Environmental Science and Engineering.
[‡] Department of Chemistry.
[§] Center for Integrated Molecular Systems.

10.1021/jp046218f CCC: $30.25
Published on Web 02/12/2005

polymerization mechanism based on our results, which would represent an overall review of the current understanding of the aniline polymerization reaction.

Experimental Section

Reagent grade nitric acid (HNO_3: Aldrich, 70%) was used as received, and aniline (Aldrich, 99.5%) was used after having been doubly distilled over zinc powder. Doubly distilled, deionized (DI) water was used for the preparation of solutions.

Polyaniline films were grown on a reflective gold disk working electrode (Olympus Co.) in a pH 0.50 HNO_3 solution containing 50 mM aniline by sweeping the potential between −0.2 and 1.05 V vs a Ag/AgCl (in saturated KCl) reference electrode. The pH of the solution was fine-controlled by adding 0.10 M KOH dropwise to a 0.30 M HNO_3 solution until desired pH was obtained when monitored with a pH meter. The working electrode was cleaned in a piranha solution (H_2SO_4: H_2O_2 = 70:30 v/v) and rinsed with DI water prior to each experiment. The working electrodes (geometric area of 0.126 cm^2) were annealed by a hydrogen flame prior to each experiment. Platinum foil and Ag/AgCl (in saturated KCl) electrodes were used as counter and reference electrodes, respectively.

Electrochemical experiments were carried out using an EG&G Princeton Applied Research model 273 (or 263A) potentiostat/galvanostat. In situ UV−vis absorption spectra were taken with an Oriel InstaSpec IV spectrometer with a charge-coupled device (CCD) array detector. The cell was configured in a reflectance mode using a bifurcated quartz optical fiber.[7] The white-light beam was brought in to the electrode surface via one branch of the bifurcated optical fiber from the light source such that the beam would be near normal to the surface. Reflected light from the electrode surface was then guided into a grating through another branch, which disperses the white beam onto the CCD array detector. The distance between the probe and the reflecting electrode was maintained at about 5 mm. A xenon lamp (75 W) was used as a light source. The wavelength of the spectrograph was calibrated using a small mercury lamp.

Synchronous and asynchronous 2D UV−vis correlation spectra were obtained using an algorithm based on a numerical method developed by Noda.[3] For the 2D correlation analysis, a subroutine named KG2D written in the Array Basic language (GRAMS/386: Galactic Inc., Salem, NH) was employed.[8] The ALS-based SMCR analysis was carried out in MATLAB (Version 6, The MathWorks). To minimize the interfering noise effect in the ALS-based SMCR operation, only the dominant four principal components obtained from principal component analysis (PCA) were used to reconstruct the spectral data and the rest were truncated as noise.

Results and Discussion

Figure 1 shows (a) a series of cyclic voltammograms (CVs) obtained during the electrochemical oxidation of 50 mM aniline in nitric acid with its pH adjusted to 0.5 and (b) the first two cyclic voltammograms singled out from the CVs shown in (a). These CVs are in excellent agreement with those reported for aniline polymerization.[1,2] As the potential increases past 0.8 V, a large anodic peak is observed for oxidation of aniline at 0.993 V at the bare gold electrode with a clear nucleation loop during the first reversal cycle, but an entirely different CV from that observed during the first cycle is obtained during the second cycle. The CV recorded during the second cycle primarily results from oxidation of dimeric species including PPD and benzidine (two middle peaks) along with an autocatalytic oxidation of aniline at about 0.92 V and a very small hint of the anodic current attributable to PAn oxidation at a potential slightly past

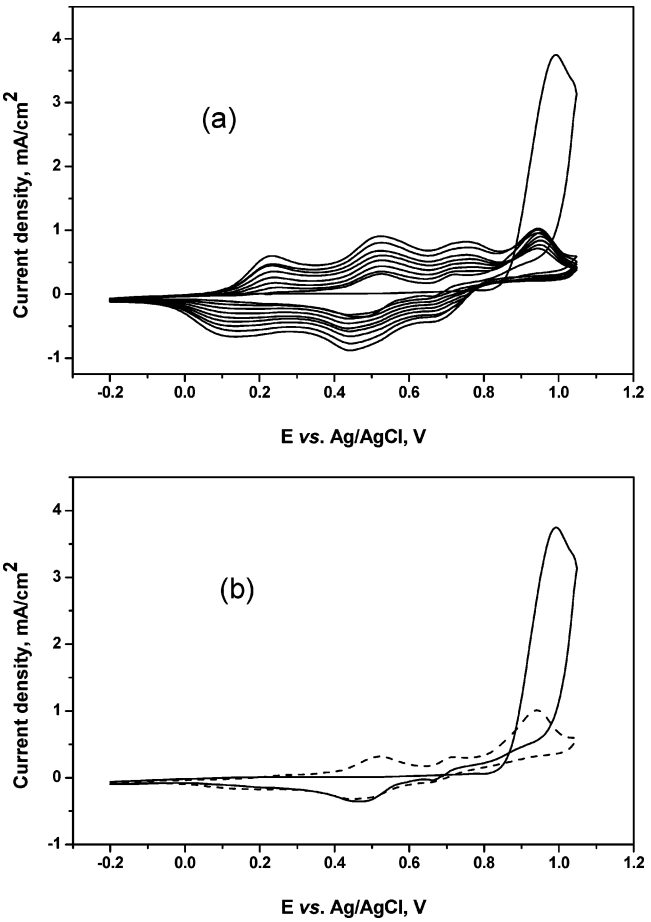

Figure 1. (a) A series of cyclic voltammograms (CVs) recorded during oxidation of 50 mM aniline in nitric acid (pH adjusted to 0.50) in a potential region between −0.20 and 1.05 V at a scan rate of 50 mV/s and (b) two first CVs singled out from (a) with the first cycle (−) and the second cycle (− − −).

SCHEME 1: Chemical Structures of Three Dimers of Aniline: (a) Benzidine, a Tail-to-Tail Dimer, (b) *N*-Phenyl-*p*-phenylene Diamine (PPD), a Head-to-Tail Dimer, and (c) Hydrazobenzene, a Head-to-Head Dimer

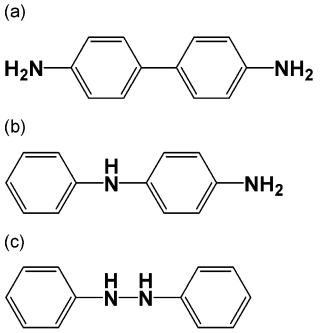

0.2 V.[2d] Electrogenerated PPD is oxidized at 0.52 V while benzidine is oxidized at 0.72 V (Figure 1b, dashed line), both with well-defined, reversible redox waves, along with a small polymer oxidation wave at about 0.20 V.[2a,b,e,g] Structures of three dimers of aniline encountered in this work are shown in Scheme 1.

Figure 2 presents two sets of a series of spectra recorded for aniline oxidation during the first (a) and the second (b) potential cycles. During the first cycle, a large increase in absorbance at 429 nm observed first accompanies two shoulder peaks at 349 and 506 nm. As the potential hits the upper limit of the anodic sweep (1.05 V) and is swept back in a reverse direction, the

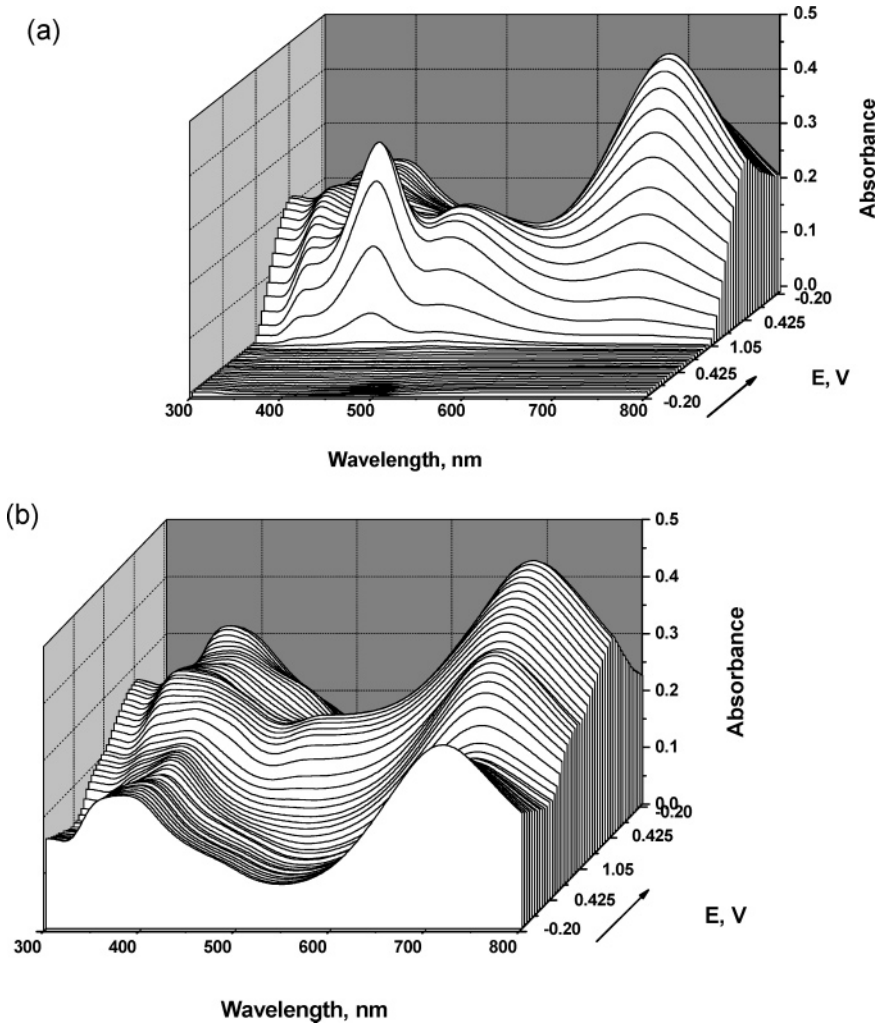

Figure 2. A series of UV−visible absorption spectra recorded concurrently with the first (a) and second (b) CVs shown in Figure 1b.

429 nm peak decreases rapidly and a number of other peaks grow and/or decay. The spectral changes become too complex to allow a straightforward interpretation to be made as the potential is reversed at the lower limit −0.20 V, where the cycle goes into the second scan. Presenting the series of spectra with a color-coded contour diagram[9] is helpful to a certain extent in taking a glance at the overall changes, but it is not only very difficult to sort out all of the spectra recorded but also impossible to keep track of each spectrum. For this reason, we ran 2D correlation analysis, which produces synchronous and asynchronous spectra.[3]

The synchronous 2D correlation spectrum represents how the variation of the spectral intensity of a band can be described in relation to those of the other bands. Cross peaks located at the off-diagonal positions of a synchronous 2D correlation spectrum represent simultaneous or coincidental changes of spectral intensities observed. Such a synchronized change suggests the possible existence of a coupled or related origin of the spectral intensity variations. The asynchronous 2D correlation spectrum represents whether any two bands undergo sequential or successive changes in their spectral intensities. An asynchronous cross peak develops only if the intensities of two spectral features change out of phase (i.e., delayed or accelerated) with each other. This feature is especially useful in differentiating overlapped bands arising from spectral signals of different origins and in determining the sequence of the spectral band emergence. Even if any given two bands are located close to each other, asynchronous cross peaks will develop between their spectral coordinates as long as the signatures or the patterns of sequential variations of spectral intensities are different.[6]

Synchronous and asynchronous 2D correlation spectra computed from the spectra shown in Figure 2a for oxidation of aniline during the first cycle are shown in Figure 3a and b, respectively. The power spectrum along the diagonal line in the synchronous spectrum is also shown on the top of Figure 3a. Autopeaks at 350, 427, 517, and 713 nm and cross peaks at (474, 350), (517, 427), (713, 350), and (713, 474−517) nm in Figure 3a show that the bands at 474, 517, and 713 nm grow together with the bands at 350, 427, and 350 as well as 474−517 nm, respectively. That is, the signs of cross peaks of the synchronous spectrum are all positive, indicating that each of them grows while the others do. The intensity of an asynchronous 2D correlation spectrum represents sequential, or successive, changes of spectral intensities measured at two frequencies, ν_1 and ν_2. An asynchronous cross peak develops only if the intensities of two spectral features change out of phase (i.e., delayed or accelerated) with each other. The sign of an asynchronous cross peak becomes positive if the intensity change at ν_1 occurs predominantly before ν_2 in the sequential order of t. It becomes negative, on the other hand, if the change occurs after ν_2. This rule, however, is reversed if the synchronous peak is negative. The analysis of the asynchronous spectrum using this rule indicates that the absorption bands emerge in the order of 427 → 474 → 517 → 350 → 713 nm. The spectrum also indicates that a new absorption peak at 474 nm, which has not been observed in the 1D power spectrum of

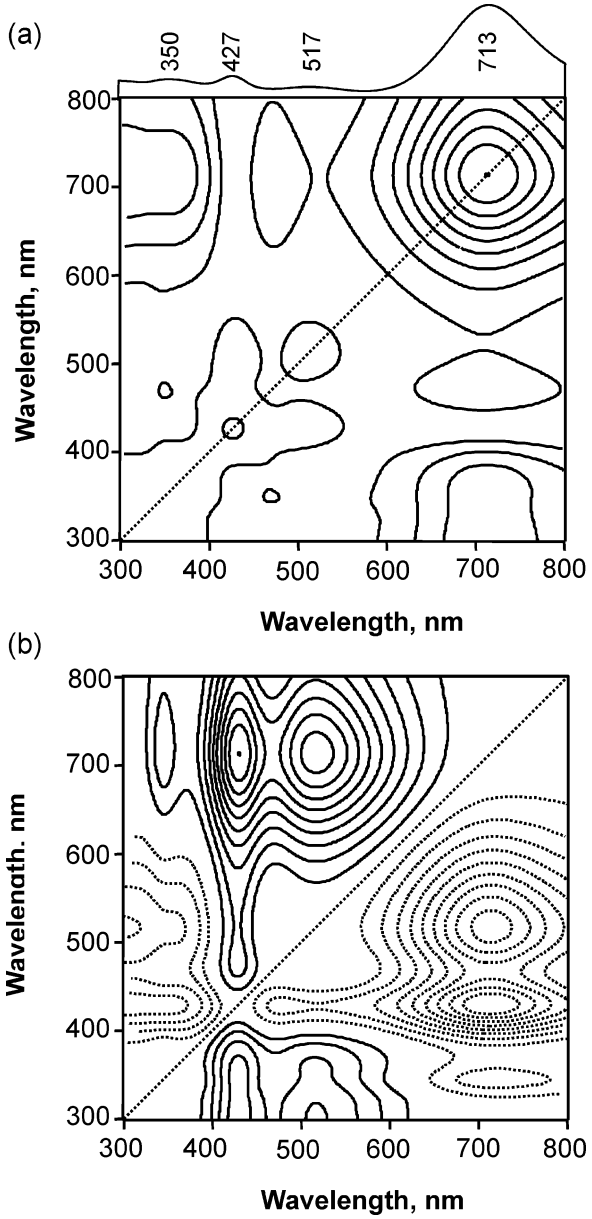

Figure 3. Two-dimensional correlation analysis of the spectra shown in Figure 2a: (a) a synchronous and (b) asynchronous correlation spectra. Solid and dashed lines represent positive and negative cross-peaks, respectively.

Figure 3a, is resolved or additionally identified. By reference to the reported spectral assignments in the literature,[2e,g] we here assign the band at 427 nm primarily to the oxidized product of the tail-to-tail dimer, that is, a benzidine quinoid; oxidized products of other dimers such as head-to-head dimer, azobenzene, and head-to-tail dimer, PPD, also absorb light at wavelengths close to this.[2e,g] Oxidized PPD was shown to absorb at about 520 and 730 nm at the beginning of its oxidation, which then shifts to about 430 nm, and the longer wavelength band becomes even stronger.[2g] This spectral change in the earlier phase of PPD oxidation was explained by an equilibrium reaction immediately following electrochemical generation of $PPD^{+\bullet}$ according to[2g]

$$2PPD^{+\bullet} \rightleftharpoons (PPD)_2 + 2H^+ \quad (1)$$

and the PPD dimer thus produced from the following reaction of $PPD^{+\bullet}$ immediately undergoes oxidation to its radical cation

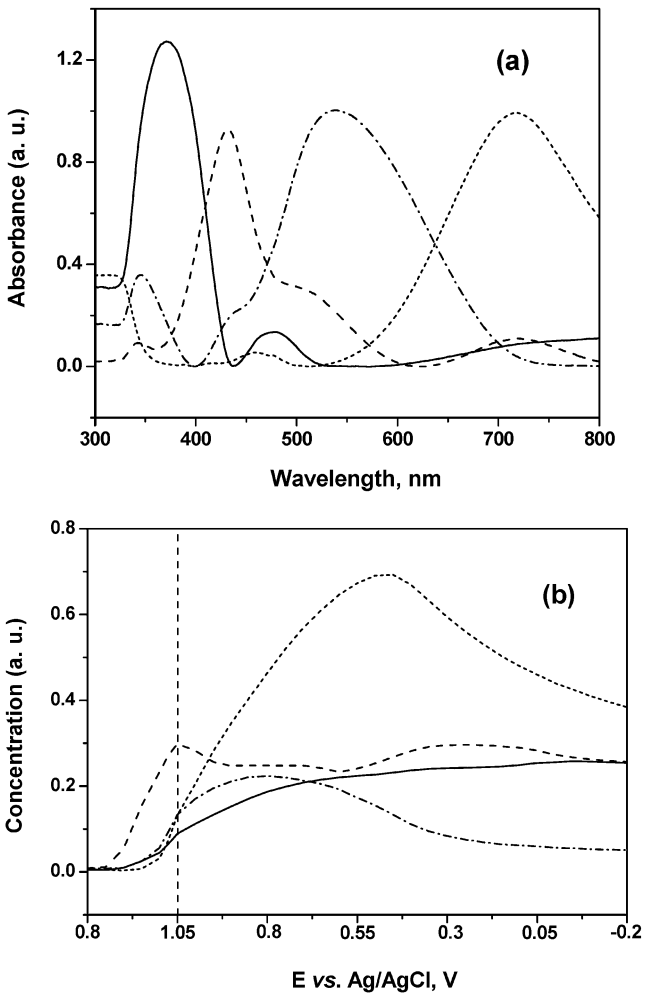

Figure 4. Pure component spectra (a) and their relative concentration profiles (b) during the first potential scan extracted from the SMCR analysis of the spectra shown in Figure 2a and the peaks identified from the asynchronous spectrum shown in Figure 3b.

by homogeneous electron transfer to other oxidized species such as the aniline cation radical or by heterogeneous electron transfer to the electrode to form $(PPD)_2^{+\bullet}$. Here, $PPD^{+\bullet}$ shows absorption bands at 430 and about 730 nm, and $(PPD)_2^{+\bullet}$ absorbs at about 530 nm and also about 730 nm as well. Thus, we can relate the absorption bands identified from the 2D correlation analysis to this equilibrium reaction, but there still are a few spectral bands whose variations are not fully explained. In other words, the interpretation of the spectral data is still difficult, although the spectral peaks are resolved and their sequence of emergence has been determined from the asynchronous spectrum shown in Figure 3b.

Based on the asynchronous cross peaks in 2D correlation analysis, the SMCR analysis has been performed for the data shown in Figure 2a, and the results are displayed in Figure 4, which shows four pure component spectra (Figure 4a) and their relative contributions to the overall spectral intensities (Figure 4b) during the potential sweep. The four components identified from reference to the spectral assignments made earlier in the related literature are the oxidized benzidine (benzidine quinoid) with its peak absorption at 432 nm (— — —),[2g] oxidized PPD with its peak absorption at 718 nm (- - - -),[2g] oxidized oligomers (radical cation of primarily the aniline tetramer or the PPD dimer) with their peak maximum at 540 nm[2g] (— - — - —), and PAn with its peak maximum at 370 nm with smaller absorbances at about 478 nm (—).[10] The neutral PAn spectrum was also

confirmed by reducing the film completely at −0.20 V for about 30 min, which had the same shape as that shown in Figure 4a as a solid line with the exception that the weaker longer wavelength absorption peaks were not observed. However, the spectrum recorded soon after the potential was stopped at −0.20 V showed longer wavelength components. The fact that all of the components except PAn are intermediate species is clearly shown by the changes in their concentration profiles (Figure 4b); all of the concentration profiles display maximum values, while that of PAn grows steadily until it becomes more or less constant below about 0.1 V during potential reversal.

There are a few points that can be made about "pure component" spectra. First, comparison of the spectrum assigned to PAn with that recorded for "pure" reduced PAn reveals that the one we extracted here has a few relatively weak additional absorption bands at 478 nm. However, the spectrum recorded for fully reduced PAn does not have these bands. This is because the doped PAn is not fully reduced upon cathodic scan to −0.20 V; it is well known that most of the conducting polymers are not reduced fully in a short time period because the diffusion of dopant ions, nitrate in this case, through the polymer film takes a long time and the polymer does not go back to a completely reduced state. For this reason, the polymer always has a small amount of doped (oxidized) state in its matrix during the potential scan and the program just does not realize the sluggish change in chemical states but recognize the summed spectrum as a pure component spectrum. We believe this might be the case for other species as well, although they would not be as serious as for PAn because the other ions or molecules are mostly smaller solution species. Second, the benzidine species is produced first upon oxidation of aniline beginning at around 0.8 V, indicating that the radical cation produced upon oxidation of aniline immediately undergoes tail-to-tail dimerization to the benzidine quinoid followed by further oxidation.

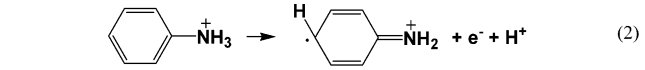

(2)

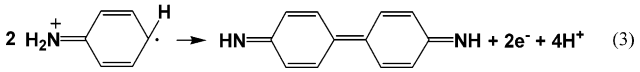

(3)

It should be pointed out, however, that the band might contain the absorbances arising from all three dimers as well. Its spectral intensity increases rapidly until it hits a maximum at around 1.05 V, where the potential is reversed. The oligomeric species, that is, primarily the aniline tetramer (− - − - −), is produced starting from about 0.9 V via dimerization of oxidized benzidine and/or the interspecies reaction between oxidized benzidine and oxidized PPD, which shows an even longer delay in its production. The PPD radical cation (- - - -) is produced rather belatedly after the benzidine concentration hits its maximum; it appears to be produced primarily via the direct coupling of the aniline radical cation and a neutral aniline molecule,[2f]

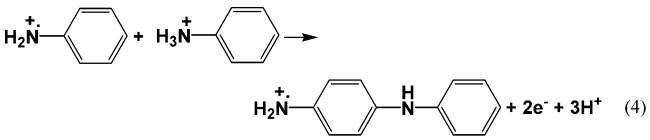

(4)

which is a resonance structure of

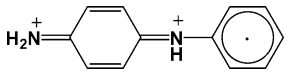

and/or the benzidine rearrangement reaction.[11] A head-to-head dimer, azobenzene, if produced, would undergo a rearrangement reaction to both the tail-to-tail dimer, benzidine, and the head-to-tail dimer, PPD. In a strongly acidic medium like this, the primary dimerization product is the tail-to-tail dimer, benzidine.[11] The two dimeric species then undergo a coupling reaction to oligomers, which undergo a further coupling reaction to the final product, PAn. These series of reactions would come to a stop when the dimers or oligomers become reduced below about 0.6 V. While the dimeric species showed their absorption at their characteristic wavelengths, the oligomeric species were shown to shift their absorption wavelengths from as short as 492 nm in the early stage of electrolysis (between 0.8 and 1.0 V during the forward scan) to eventually 540 nm in the later stage (between 0.90 and 0.60 V during the reverse scan), when the segments of a few relatively narrow potential regions were analyzed (not shown). This indicates that the conjugation length of the oligomer grows during the potential scan due to the coupling reaction and grows eventually to what is regarded as PAn.

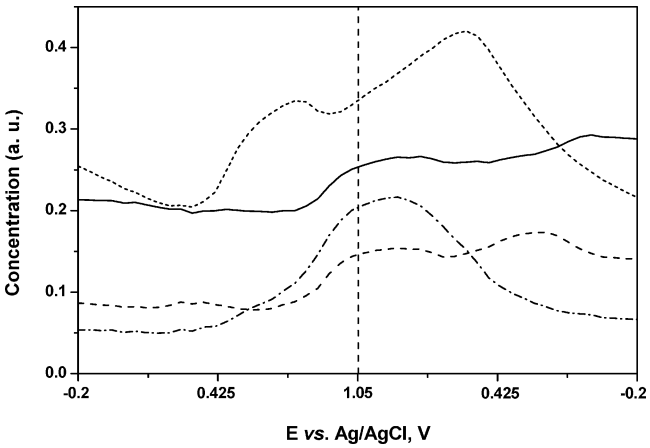

Figure 5. Relative concentration profiles obtained during the second potential scan.

The result of this analysis becomes even more convincing when we take a look at the second potential scan. Examining the second CV scan shown as a dashed line in Figure 1b, we realize that the primary species undergoing oxidation upon anodic scan are the dimeric species oxidized at 0.52 (PPD) and 0.72 V (benzidine) before the potential becomes positive enough to autocatalytically oxidize aniline.[2d] As was pointed out already, there is a small anodic current arising from PAn oxidation starting at around 0.2 V, which has been produced from aniline oxidation during the first complete potential scan. Now the concentration profiles obtained to the end of the second potential scan displayed in Figure 5 show more or less patterns similar to those shown in Figure 4b except that the benzidine quinoid shows a steady-state concentration until the potential reaches about 0.9 V while the PPD radical cation shows a rather fast increase from about 0.45 V but the increase slows down starting from about 0.58 V, which then peaks out at about 0.75 V and starts to increase again from about 0.9 V until it reaches the maximum at about 0.55 V during the reversal scan. In the meantime, the oligomeric species begins to be produced from about 0.43 V and reaches its maximum at about 0.9 V during the reversal potential sweep. These observations are explained by the fact that the oxidized PPD species is produced when the electrode potential reaches around 0.42 V, where the neutral PPD produced from reduction of its cation radical or dication during the reversal scan is reoxidized. The slight increase in the benzidine quinoid concentration, however, is observed above about 0.7 V due to its higher oxidation potential, and the rate

of its increase becomes significant only when aniline oxidation results in generation of the benzidine species above about 0.9 V. The increases and decreases in the oligomer concentrations along with the change in potential generally follow the increases in dimer concentrations; this is consistent with their generation via coupling of monomeric and dimeric species following aniline oxidation.

When it comes to the 10th cycle, however, the system becomes much more complex. The complexity arises from the fact that a few more spectral components are added to the already complex four-component system as PAn itself generates various forms of oxidized states with their own spectra during the anodic scan.[10] To make the situation worse, the absorption bands assigned to the polaron (radical cation), the bipolaron (dication), and the quinoidal form of PAn resemble the absorption bands from the benzidine quinoid, $PPD^{+\bullet}$, and oxidized oligomers, respectively. As a result, our software program becomes incapable of resolving the spectra. For this reason, we did not carry out further analyses beyond the third cycle. Nevertheless, dimers are still generated as can be seen from the increase in the reversal CV peaks shown in Figure 1a, and we believe that essentially the same process as we have seen during the first and second potential scans takes place along with the polymer oxidation starting from about 0.1 V, which is now clearly seen.

As a final proof of concept, we also compared the rates of generation of the intermediate species computed from the concentration profiles in Figure 5 with the corresponding derivative cyclic voltabsorptometric (DCVA) signals.[7b,c] The concentrations obtained from the SMCR fitting were used for the calculation of rates, while the DCVA signals were obtained from the spectra shown in Figure 2 by simply taking the derivative signals with respect to time at selected wavelengths.[7b,c] If a wavelength picked is well resolved from others representing a given species, the above two signals should coincide with each other when they are normalized with respect to their peak signals because the absorbance is directly proportional to the concentration. Figure 6 shows the rate of generation in terms of the d*C*/d*t* (a) and d*A*/d*t* signals (b), both obtained during the second potential cycle, with a provision that the 370 nm peak represents neutral PAn (−), the 432 nm peak the benzidine quinoid (− − −), the 540 nm peak the oxidized oligomer (− - − - −), and the 718 nm peak the PPD cation radical (- - - -). It can be seen from Figure 6a and b that the rates of generation of each species plotted as a function of potential are very similar to each other. This indicates that the SMCR-extracted spectra and their concentration profiles do indeed represent valid physical characteristics of the products and intermediate species electrogenerated. However, a close examination of the rates expressed in terms of d*C*/d*t* and d*A*/d*t* reveals that the d*A*/d*t* signals generally show broader ranges of potentials for the same amount of changes as for the corresponding d*C*/d*t* signals, indicating that the absorbance signals are not resolved as well as the d*C*/d*t* signals. This is readily seen from the spectra shown in Figure 4a, in which the 370 nm band, for example, is made of a major absorption band of neutral PAn with two minor absorption bands arising from the benzidine quinoid and the oligomer bands. Other bands have similar problems. For this reason, the d*A*/d*t* signal generally has a wider potential range for its change than the d*C*/d*t* signal does. Thus, we conclude that the d*C*/d*t* computed from the concentration profiles represents a more correct rate of generation or destruction.

During the second potential cycle (Figure 6), the rate of generation of the PPD cation radical is negative at the beginning

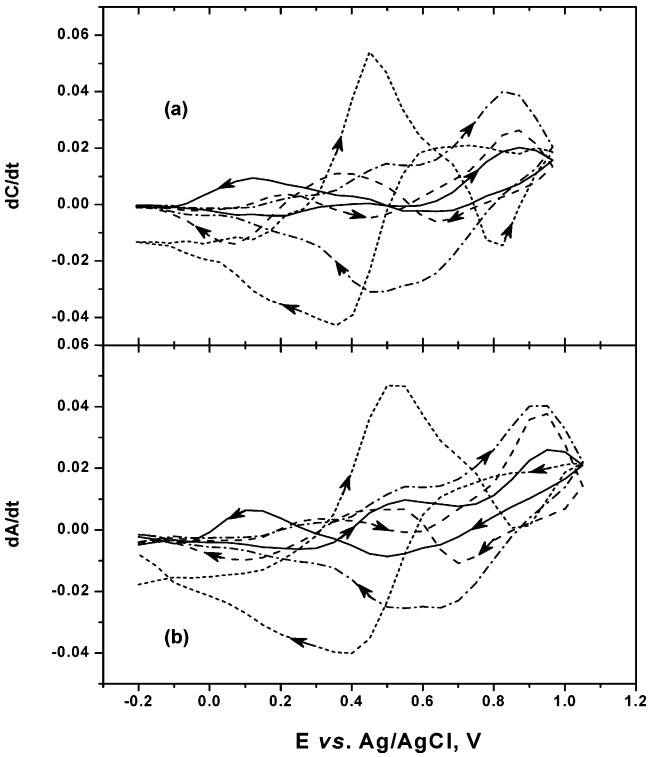

Figure 6. (a) d*C*/d*t* versus *E* plot obtained from the concentration profiles shown in Figure 5 and (b) d*A*/d*t* versus *E* plot calculated from the data shown in Figure 2b.

of the second potential scan, becomes positive slightly below 0.4 V, and peaks out at about 0.45 V. The rate of generation then decreases rapidly for perhaps two reasons: the first is its further oxidation to the dication because of the increased electrode potential,[2g] and the second is its dimerization to the aniline tetramer. The rapid decrease in the rate of generation of this species is accompanied by an increase in the rate of generation of the oxidized oligomer, which indicates that the dimerization reaction of the radical cation is largely responsible for its rapid decrease. The most peculiar behavior is shown by the benzidine quinoid, which begins to be generated from as low a potential as 0.15 V, peaks out at about 0.25 V, hits a minimum at about 0.5 V, and then increases again rather rapidly. The increase in its rate of generation in the potential range of about 0.5−0.7 V is due to the oxidation of reduced benzidine produced in the first cycle during the reverse potential scan. The rather rapid increase beyond about 0.8 V is obviously due to the autocatalytic oxidation of aniline to its radical cation, followed by dimerization to the benzidine quinoid according to reaction 3.[2d] However, the increase and decrease in the concentration of this species shown between 0.15 and 0.5 V are difficult to understand; perhaps the oxidation of a small amount of the neutral polymer to its radical cation (polaron) might have contributed to this behavior also.[10] The first small decrease in the amount of neutral PAn between 0.0 and 0.25 V upon anodic scanning along with the small increase in the 432 nm band (benzidine quinoid) supports this explanation. The amount of neutral PAn then starts to increase from about 0.3 V, which is accompanied by increases in both the PPD cation radical and the oxidized oligomer. It then increases rather steeply from about 0.7 V until it goes through the maximum at about 0.9 V; this rather rapid increase is accompanied by the decrease in the PPD radical cation concentration and increases in concentrations of the oxidized oligomer and the benzidine quinoid. From these observations, we conclude that PAn grows

primarily via coupling of oxidized dimers and oligomers after the formation of PPD, the benzidine quinoid, and/or the oligomers.

The 2D correlation spectral analysis here allows the polymerization mechanism to be constructed. The mechanisms proposed for the aniline polymerization in the literature were primarily based on analysis of electrolysis products,[2a,b] CV current analysis,[2f] impedance analysis,[12] and spectroelectrochemical experiments.[2c,e,g] Although the spectroelectrochemical experiments provided the most convincing evidence for intermediate species, the conclusion is usually reached from the coincidence of the absorption peaks with those of suspected intermediate species. However, the spectral changes taking place are much too complex as can be seen from Figure 2, and it is practically impossible to specifically pin down the changes taking place due to specific components. In our analysis, the pure component spectra have been extracted and their behaviors traced as a function of potential scanned, which provides a full scenario for the reaction.

Conclusions

We have demonstrated in this study that the complex spectra obtained during an experiment, in which an external perturbation is applied, can be resolved into component spectra and their concentration profiles can be constructed employing 2D correlation spectroscopy and SMCR analyses. While the external perturbation was the potential in our study, it could be any other experimental parameters. Our 2D correlation analysis and SMCR study on a series of spectra obtained during aniline oxidation in nitric acid at pH = 0.50 not only positively identified and confirmed all of the spectra of intermediate species proposed in the literature but also showed how the concentrations of intermediate species varied as a function of the scanned potential. To our knowledge, this is the first complete analysis of the complex spectra obtained during aniline oxidation, although numerous studies have been reported on the reaction. A conclusion has been reached from the variation of the concentration of a species on whether it is an intermediate species or a final product. The mechanism constructed from our results represents an overall summary of the state-of-the-art understanding of the aniline polymerization reaction. The technique introduced in our study would certainly open a way for studying complex electrochemical reactions including polymerization reactions, in which highly convoluted spectra are obtained with a variation of an external perturbation.

Acknowledgment. This work was supported by the Korea Science and Engineering Foundation through the Center for Integrated Molecular Systems located at the Pohang University of Science and Technology. Post- and pregraduate stipends have been provided by the BK-21 program of the Korea Research Foundation.

References and Notes

(1) See review articles among many others such as: (a) Trivedi, D. C. In *Handbook of Organic Conductive Molecules and Polymers*; Nalwa, H. S., Ed.; John Wiley & Sons Ltd.: Chichester, England, 1997; Vol. 2. (b) Park, S.-M. In *Handbook of Organic Conductive Molecules and Polymers*; Nalwa, H. S., Ed.; John Wiley & Sons Ltd.: Chichester, England, 1997; Vol. 3. (c) Hugot-Le-Goff, A. In *Handbook of Organic Conductive Molecules and Polymers*; Nalwa, H. S., Ed.; John Wiley & Sons Ltd.: Chichester, England, 1997; Vol. 3.

(2) (a) Mohilner, D. M.; Adams, R. N.; Argersinger, W. J. *J. Am. Chem. Soc*. **1962**, *84*, 3618. (b) Bacon, J.; Adams, R. N. *J. Am. Chem. Soc*. **1968**, *90*, 6596. (c) Genies, E. M.; Lapkowski, M. *J. Electroanal. Chem*. **1987**, *236*, 189. (d) Stilwell, D. E.; Park, S.-M. *J. Electrochem. Soc*. **1988**, *135*, 2254. (e) Shim, Y.-B.; Won, M.-S.; Park, S.-M. *J. Electrochem. Soc*. **1990**, *137*, 538. (f) Yang, H.; Bard, A. J. *J. Electroanal. Chem*. **1992**, *339*, 423. (g) Johnson, B. J.; Park, S.-M. *J. Electrochem. Soc*. **1996**, *143*, 1277.

(3) (a) Noda, I. *Appl. Spectrosc*. **1993**, *47*, 1329. (b) Noda, I.; Dowrey, A. E.; Marcott, C.; Story, G. M.; Ozaki, Y. *Appl. Spectrosc*. **2000**, *54*, 236A−248A. (c) Noda, I. *Appl. Spectrosc*. **2000**, *54*, 994.

(4) Jung, Y. M.; Noda, I.; Kim, S. B. *Appl. Spectrosc*. **2003**, *57*, 1376.

(5) (a) Gillie, J. K.; Hochlowski, J.; Arbuckle-Keil, G. A. *Anal. Chem*. **2000**, *72*, 71R. (b) Noda, I. In *Handbook of Vibrational Spectroscopy*; Chalmers J. M., Grtiffiths, P. R., Eds.; Wiley & Sons Ltd.: New York, 2002; Vol. 3, pp 2123−2134. (c) Jung, Y. M.; Czarnik-Matusewicz, B.; Ozaki, Y. *J. Phys. Chem. B* **2000**, *104*, 7812. (d) Izawa, K.; Ogasawara, T.; Masuda, H.; Okabayashi, H.; O'Connor C. J.; Noda, I. *J. Phys. Chem. B* **2002**, *106*, 2867. (e) Shin, H. S.; Jung, Y. M.; Lee, J.; Chang, T.; Ozaki, Y.; Kim, S. B. *Langmuir* **2002**, *18*, 5523. (f) Eads, C. D.; Noda, I. *J. Am. Chem. Soc*. **2002**, *124*, 1111. (g) Choi, H. C.; Jung, Y. M.; Noda, I.; Kim, S. B. *J. Phys. Chem. B* **2003**, *107*, 5806.

(6) Kim, Y.-O.; Jung, Y. M.; Kim, S. B.; Park, S.-M. *Anal. Chem*. **2004**, *76*, 5236.

(7) (a) Pyun, C.-H.; Park, S.-M. *Anal. Chem*. **1986**, *58*, 251. (b) Zhang, C.; Park, S.-M. *Anal. Chem*. **1988**, *60*, 1639. (c) Zhang, C.; Park, S.-M. *Bull. Kor. Chem. Soc*. **1989**, *10*, 302.

(8) The program can be downloaded from the homepage of Prof. Yukihiro Ozaki of Kwansei Gakuin University, Japan (http://science.kwansei.ac.jp/;ozaki/).

(9) Shim, H.-S.; Yeo, I.-H.; Park, S.-M. *Anal. Chem*. **2002**, *74*, 3540.

(10) (a) Stilwell, D. E.; Park, S.-M. *J. Electrochem. Soc*. **1989**, *136*, 427. (b) Genies, E. M.; Lapkowsky, M. *J. Electroanal. Chem*. **1987**, *220*, 67. (c) Cushman, R. J.; McManus, P. M.; Yang, S. C. *J. Electroanal. Chem*. **1987**, *219*, 335. (d) McManus, P. M.; Cushman, R. J.; Yang, S. C. *J. Phys. Chem*. **1987**, *91*, 1575.

(11) Gould, E. S. *Mechanism and Structure in Organic Chemistry*; Holt, Rinehart and Winston: New York, 1959; pp 656−661.

(12) (a) Johnson, B. J.; Park, S.-M. *J. Electrochem. Soc*. **1996**, *143*, 1209. (b) Yoo, J.-S.; Song, I.; Lee, J.-H.; Park, S.-M. *Anal. Chem*. **2003**, *75*, 3294.